
CONVOLUTIONAL NEURAL NETWORKS AS SUMMARY STATISTICS FOR APPROXIMATE BAYESIAN COMPUTATION

A PREPRINT

Mattias Åkesson*, Prashant Singh, Fredrik Wrede, Andreas Hellander

Department of Information Technology

Division of Scientific Computing

Uppsala University

SE 751 05 Uppsala, Sweden

andreas.hellander@it.uu.se

June 6, 2022

ABSTRACT

Approximate Bayesian Computation is widely used in systems biology for inferring parameters in stochastic gene regulatory network models. Its performance hinges critically on the ability to summarize high-dimensional system responses such as time series into a few informative, low-dimensional summary statistics. The quality of those statistics acutely impacts the accuracy of the inference task. Existing methods to select the best subset out of a pool of candidate statistics do not scale well with large pools of several tens to hundreds of candidate statistics. Since high quality statistics are imperative for good performance, this becomes a serious bottleneck when performing inference on complex and high-dimensional problems. This paper proposes a convolutional neural network architecture for automatically learning informative summary statistics of temporal responses. We show that the proposed network can effectively circumvent the statistics selection problem of the preprocessing step for ABC inference. The proposed approach is demonstrated on a benchmark problem and a challenging inference problem learning parameters in a high-dimensional stochastic genetic oscillator. We also study the impact of experimental design on network performance by comparing different data richness and data acquisition strategies.

Keywords Likelihood-free inference · Summary statistics · Convolutional neural networks · Approximate Bayesian computation · Feature selection

1 Introduction

Likelihood-free parameter inference is a well-studied problem encountered in various domains, most notably including computational biology and astrophysics. The parameter inference problem involves fitting the parameters of a simulation or analytical model to observed data from real-world experiments or measurements. This allows effective use of simulation models for deeper analysis and understanding of the physical phenomena behind the observed data. The most straight-forward way of estimating parameters in this setting is using methods like maximum likelihood-estimation. However, one rarely knows the form of the likelihood function in the case of simulation models. For most practical purposes, likelihood-free parameter inference is the norm. Approximate Bayesian computation (ABC) [1, 8] has established itself as the most popular likelihood-free inference (LFI) method in the recent past, owing to its flexibility and demonstrated performance on a variety of problems.

Although ABC is a robust LFI method, it involves substantial hyperparameter optimization which makes it challenging to set up optimally [11, 8], particularly for complex high-dimensional LFI problems involving tens of parameters. The choice of summary statistics is a hyperparameter that presents a great challenge to set up effectively. Summary statistics are typically hand-picked by the practitioner. There exist automated summary statistic selection methods but

*now at Scaleout Systems AB.

existing approaches scale poorly as the number of candidate summary statistics in the pool increases. Furthermore, optimal summary statistics may not even be present in the initial candidate pool, which may lead to sub-optimal inference quality.

Therefore, there has been great interest in developing methods that alleviate cumbersome and explicit summary statistic selection. Kernel embeddings have been explored within the ABC framework to directly compare observed and simulated data by means of a maximum mean discrepancy measure [9]. Fearnhead and Prangle [3] show that the best choice for a summary statistic is the posterior mean, when minimizing the quadratic loss. Building upon this theme, recent methods of interest involve training machine learning (ML) regression models using training data X that learn the posterior mean $E(\theta | X)$ of parameters θ [10, 6, 13]. The training data X is composed of pairs $(f(\theta), \theta)$, where θ are sampled from a *prior* distribution $p(\theta)$. The resulting regressor $\hat{\theta}(X)$ captures various characteristics of X and can be used as a summary statistic within the ABC framework.

This paper proposes a convolutional neural network (CNN) architecture that learns the estimated posterior mean $\hat{\theta}(X)$. The CNN is particularly effective towards learning local features that can distinctly characterize various intricate patterns within time series responses. This allows for more accurate modeling of the posterior mean, and in turn enhances inference quality. Section 2 formally introduces the likelihood-free parameter inference problem, and briefly describes existing methods, including ABC and artificial neural network (ANN) based methods. Section 3 briefly explains CNNs and presents the proposed CNN architecture for learning summary statistics. Section 4 describes the experimental settings and Section 5 demonstrates the performance of the proposed approach on test problems, and compares the results with the state of the art. Section 6 concludes the paper.

2 Background and Related Work

Consider an observed dataset X and a simulator or analytical model $f(\theta)$ corresponding to the physical process that generated X . The parameter inference task in a likelihood-free setting is to infer the value of parameters θ that results in simulator output $f(\theta)$ agreeing with observed data X . As inference in a likelihood-free setting must proceed solely using access to the simulator $f(\theta)$ and observed dataset X , sampling candidate θ and comparing simulated responses to X forms the basis of ABC. The ABC *rejection sampling* algorithm begins by sampling candidate $\theta \sim p(\theta)$, where $p(\theta)$ represents a *prior* function encoding prior knowledge about the problem. The sampled θ is then simulated and the response $\mathbf{y} = f(\theta)$ is compared to X . As these quantities are typically high dimensional, the comparisons are made in terms of low-dimensional features or *summary statistics* $\mathbf{S} = \{S_1(\mathbf{y}), \dots, S_n(\mathbf{y})\}$ of high-dimensional responses. The simulated response \mathbf{y} can then be compared to X using a distance function d as $d_{sim} = d(\mathbf{S}(\mathbf{y}), \mathbf{S}(X))$. Given a tolerance threshold τ , if $d_{sim} \leq \tau$, then the corresponding θ is deemed to be accepted, else rejected. This rejection sampling cycle proceeds until a specified number of samples have been accepted, forming the estimated posterior.

As the summary statistics form the basis of the comparison between simulated responses and observed data, the choice and subsequent quality of used statistics is paramount towards achieving high quality inference. Substantial effort has been invested in research towards summary statistic selection [11][Chap. 5], yet existing methods do not scale well for high-dimensional problems and can be hard to setup correctly. In most practical applications, practitioners typically hand-pick a small number of summary statistics, which may not be optimal. Therefore, recent advances in automating summary statistic selection using regression models are of particular interest, and are discussed below.

2.1 Estimated posterior mean as a summary statistic

Fearnhead and Prangle [3] presented a regression-based approach towards constructing summary statistics where, for $\theta_j, j = 1, \dots, L$, a linear regression model of the form,

$$\theta_j^i = E(\theta_j | \mathbf{y}^i) = b_0 + b_j h(\mathbf{y}^i) + \xi^i, \quad (1)$$

with \mathbf{y}_i being the i -th simulated sample or observed data sample and ξ^i is Gaussian mean-zero noise. The parameters in the equation above are fitted using least-squares on a training set or dataset D of N pairs $D = (\theta^i, \mathbf{y}^i), \theta \sim p(\theta)$. The estimated mean posterior represented by the L linear regression models can then be used as a summary statistic within ABC rejection sampling. The dataset D makes use of $p(\theta)$ but is distinct from rejection sampling. Therefore, the statistic selection process entails significant overhead.

A useful modification to the way ABC is performed also helps in achieving better data efficiency. The training set D of N pairs (θ^i, \mathbf{y}^i) is used to train the regressor, but is also used to perform ABC in a *reference table* scenario as in [2]. The reference table method entails computation of N distance values $d_{sim}^i = \{d(\mathbf{S}(\mathbf{y}^i), \mathbf{S}(X))\}_{i=1}^N$ for the N samples originating from the prior p and comprising the dataset D . The samples comprising the smallest x -th percentile of all distances are deemed to be accepted samples and form the ABC estimated posterior. The reference

table method allows for reusing training data in subsequent ABC rejection sampling, enabling better data efficiency. The ABC reference table method is used in the ANN based methods described below, and also in this work.

Deep neural networks were proposed to estimate the posterior mean by Jiang et al. [6] as a more powerful method to learn informative summary statistics as compared to linear regression. The dense (deep) neural network (DNN) model is the simplest ANN model, it consists of multiple layers of interconnected neurons. The DNN based summary statistic construction in [6] was shown to outperform the linear regression method, though at additional computational cost as the DNN requires more voluminous training data.

A novel ANN architecture named partially exchangeable networks (PEN) was proposed by Wqvist et al. [13]. The model is an generalization of the Deep Sets model [14], an ANN model using sets instead of ordered data as input. The PEN model extends the idea of sets for data with d -partially exchangeable structures in a conditionally Markovian context. The authors show results for 4 different stochastic models, where two of the examples are time series: the regression model of order 2 and the Moving Average of order 2 also used in [6]. The results shows that the PEN models produce a more reliable posterior even when using less training data compared to the DNN.

Although the PEN architecture reduces the number of trainable weights of the ANN (and in turn increases ANN model efficiency) by leveraging partial exchangeability, we believe there is room to improve the expressive power of the ANN model by exploiting rich local patterns present within temporal responses. We propose a general convolutional neural network (CNN) architecture wherein a sequence of convolutional layers extracts specific local patterns within the input time series. These rich local patterns allow the CNN model to incorporate effective discriminative abilities for input patterns, that are critical in an informative summary statistic. The aim of this work is therefore to develop a CNN architecture that exceeds current state of the art ANN summary statistic models in terms of informativeness and subsequent ABC inference quality for complex large-scale problems, while being data-efficient. The following section explores our proposed CNN architecture in detail.

3 Convolutional Neural Networks as Summary Statistics

The inherent structure in time series makes convolutional networks an attractive option to explore for the task of learning the mapping between time series responses as input to the CNN, and the posterior mean $\hat{\theta}$ as output of the CNN. The CNN will effectively incorporate summary statistics in its hidden layers and can subsequently be used in conjunction with existing likelihood-free inference methods for parameter inference, or to perform model exploration where the goal is to screen the parameter space for different qualitative behaviors produced by the model.

Convolutional neural networks (CNN) form an architecture of neural networks for processing data having a grid-based structure. Temporal data in the form of time series is often obtained at regular intervals, forming a 1-dimensional grid structure. This is certainly true for time series data originating from simulations where it is possible to have time series values at specific time points. This property makes CNNs particularly suited for estimating the posterior mean and the input patterns are time series sampled at regular intervals.

A CNN replaces general matrix multiplication in a multi-layer neural network with the convolution operation in at least one of the layers. The convolution operation enables performing weighted averaging of inputs such that more recent entities in the input are given larger weights. Intuitively, this allows for identification of local informative patterns in data. For example, in case of time series as input, the convolution operation can be used to identify distinct behaviors such as maxima, distance to first peak, etc. No hand-crafting of features is necessary. Formally, for input data y and a kernel w , the discrete convolution operator can be defined as follows [5],

$$s(t) = (y * w)(t) = \sum_{-\infty}^{\infty} y(a)w(t - a), \quad (2)$$

where t is a specific time point. The kernel w is essentially a filter represented by a matrix of trainable weights. The kernel matrix is typically small and is applied to a small region of the input. By operating as a filter, the kernel is able to enable detection of features such as edges of objects within an image. In case of time series, such features would include various characteristics of the time series such as distinct types of peaks.

Figure 1 depicts the CNN architecture used for experiments in this article concerning the genetic oscillator test problem described later. The input layer of dimensionality (401×1) accepts the time series input, where each time series is composed of 401 values. A sequence of convolutional and pooling layers then operate on the time series where the convolution operator identifies local patterns in the input to the layer, and subsequently the pooling operation replaces the output at certain places with a feature of nearby outputs. Specifically, we use max pool [15] where the maximum value of the output within a rectangular neighborhood is chosen [5]. The pooling layer thus achieves dimensionality reduction or in essence, feature selection from the convolution layer where it receives input from. The effect of

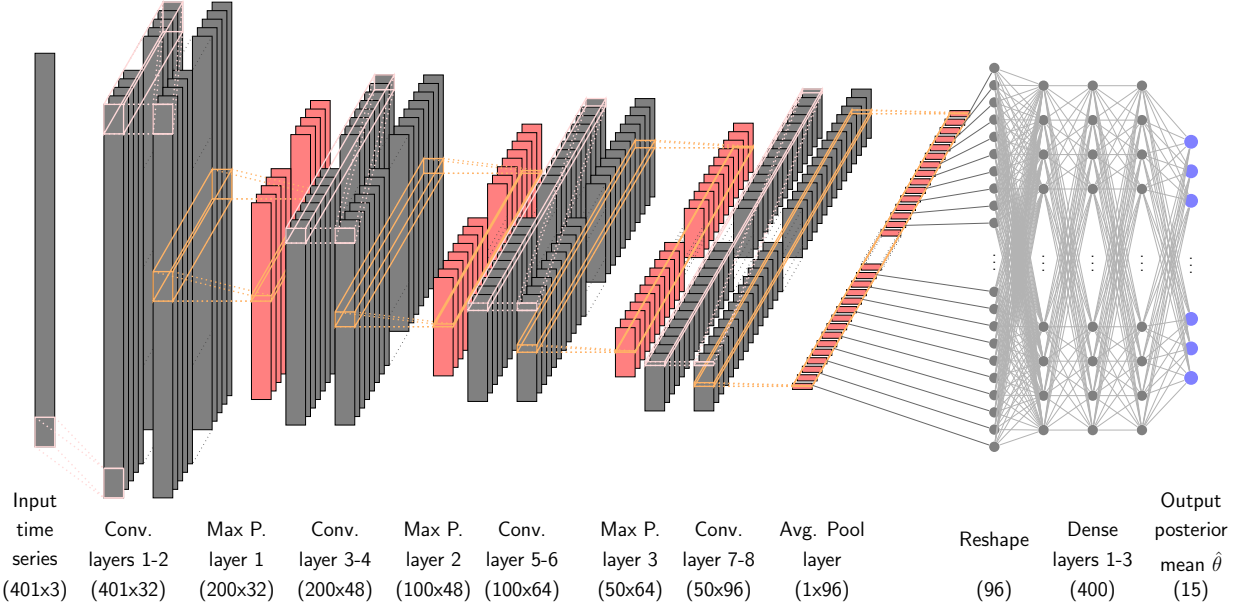


Figure 1: A schematic view of the neural network used in this work for the genetic oscillator test problem. Pink connections visualize convolutional operations, orange connections visualize max pooling operations.

pooling is also that the size of the network decreases, reducing the computational complexity. After 3 combinations of convolution and max pooling, the output is processed through a layer of average pooling and subsequently through 3 dense layers before finally reaching the output layer representing the estimated posterior mean.

4 Experimental Setup

As a very popular use case of summary statistics lies within likelihood-free inference algorithms, experiments are designed to evaluate the informativeness of the CNN-based summary statistic in the context of ABC parameter inference. The proposed CNN architecture is evaluated and compared to the DNN [6] and PEN [13] architectures. The term ANN is used henceforth to refer to either of the DNN, PEN and CNN architectures. The likelihood-free parameter inference pipeline using the ANN-based summary statistics consists of the following steps.

1. Generate training data for the ANN: draw N samples from a uniform prior defined over a specified range, and simulate the corresponding time series.
2. The ANN regression model is trained on the N samples above, and is used to predict the posterior mean for some observed data.
3. ABC inference: the predicted posterior mean is used as a summary statistic within the framework of ABC rejection sampling. The reference table method described earlier is used in the experiments, and utilizes pre-generated data. The rejection sampling method with pre-generated data is equivalent to the k-Nearest Neighbour (k-NN) algorithm.

The following text describes the experimental setup with respect to quantifying the summary statistic posterior estimation error, and the ANN model training framework.

4.1 Summary Statistic Posterior Estimation Error

In order to evaluate the goodness of ANN-based summary statistics, the quantity of expected distance can be defined as follows,

$$\mathbb{E}_{\theta \in p(\theta)} \approx D(\hat{\theta}, \theta), \quad (3)$$

where $\hat{\theta}$ is the posterior mean estimated by the ANN model, θ represents the true parameter values and D is a given distance function. The expected distance is proportional to the entropy of the approximated posterior given by the

ANN model and therefore computing the expected distance as in Eq. (3) provides a measurement of the estimation error of the summary statistic.

A measure independent of the considered prior range is desirable. Thereto, the normalized mean absolute error (MAE) is defined as,

$$E_{\%} = \frac{\mathbb{E}_{\theta \in p(\theta)} |\theta - \hat{\theta}|}{\mathbb{E}_{\theta \in p(\theta)} |\theta - \theta_m|}, \quad (4)$$

where the denominator is the expected optimal guessing MAE based on the prior knowledge, i.e. the prior mean θ_m . This allows capturing the new information gained by the regression-based ANN models over the prior knowledge. $E_{\%} = 1$ indicates no new information gained while $E_{\%} < 1$ indicates relative accuracy improvements or new information gained by the regression model. A uniform prior $U(\mathbf{dmin}, \mathbf{dmax})$ is used, resulting in the denominator taking the form,

$$\mathbb{E}_{\theta \in p(\theta)} |\theta - \theta_m| = \frac{\mathbf{dmax} - \mathbf{dmin}}{4}. \quad (5)$$

The numerator can be approximated using a set of n test points as,

$$E_{\theta \in p(\theta)} |\theta - \hat{\theta}| \approx \frac{1}{n} \sum_{i=1:n} |\theta_i - \hat{\theta}_i|. \quad (6)$$

Equation (4) can now be rewritten as,

$$E_{\%} \approx \frac{4}{\mathbf{dmax} - \mathbf{dmin}} \frac{1}{n} \sum_{i=1:n} |\theta_i - \hat{\theta}_i|. \quad (7)$$

4.2 Model Training

The training data corresponding to the DNN, PEN and CNN models is pre-computed and is the same for all three architectures for a given experiment. The training data consists of $N = 300,000$ samples, with a validation set of 20,000 samples and a test set of 100,000 samples for the genetic oscillator test problem. Each of the 100,000 test samples is treated as an observed dataset.

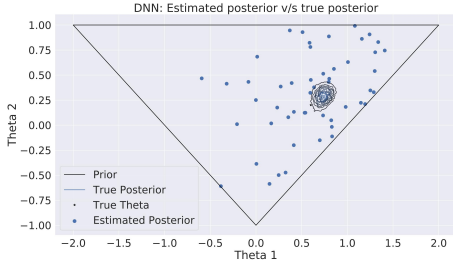
The models are trained in two stages involving two different batch sizes of training data. In the first stage, a relatively small batch size of 32 is used and stochastic gradient descent is used to optimize the ANN model hyperparameters. The numbers of training epochs is determined by the early stopping regularization with the patience parameter being 5 epochs. In the second stage, a batch size of 4096 is used, along with the same early stopping criterion described above. The loss function for model training is mean squared error (MSE) on the training set, while the early stopping criterion involves calculation of the mean absolute error (MAE) using the validation set. The test set is finally used to calculate the expected estimation distance as in Eq. (3).

5 Results

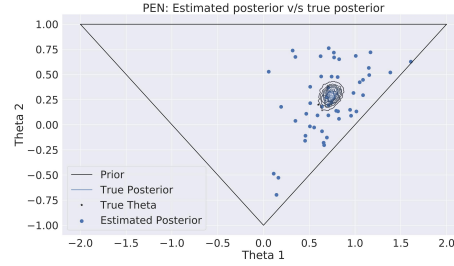
The proposed approach is demonstrated on two test problems. The moving average 2 (MA2) model is a benchmark parameter inference test problem in literature, and serves to effectively compare the proposed approach to existing methods. The genetic oscillator is a challenging high dimensional test problem and serves to demonstrate the scalability of the proposed approach.

5.1 The Moving Average 2 Model

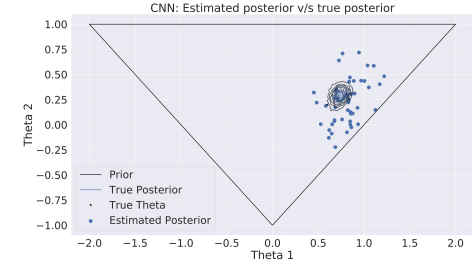
The moving average model is a relatively simple and popular benchmark example used in ABC [8] and ANN summary statistics literature [6, 13]. The typical model setting considered herein (and in works above) allows exact calculation of the posterior distribution. Manually selected summary statistics for the moving average model include autocovariance at various lag intervals, and have been extensively studied [8, 13]. The moving average model is therefore a good choice for benchmarking new summary statistic selection methods in an ABC context. The experimental settings follow [13].



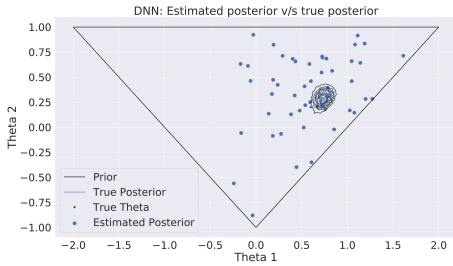
(a) DNN - training set of 1000 samples.



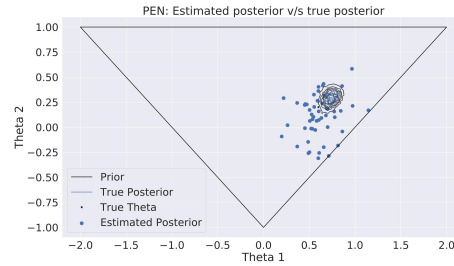
(b) PEN - training set of 1000 samples.



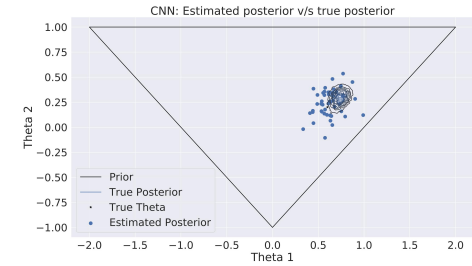
(c) CNN - training set of 1000 samples.



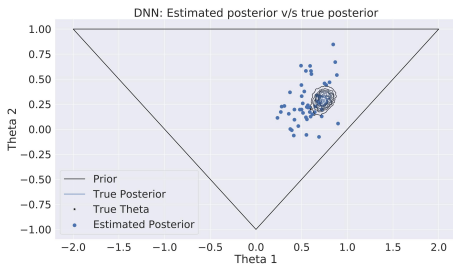
(d) DNN - training set of 10000 samples.



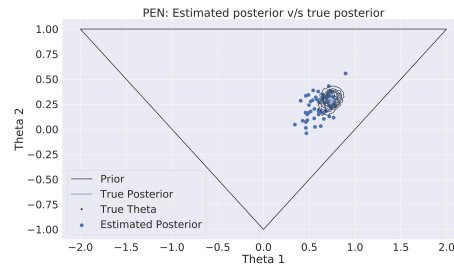
(e) PEN - training set of 10000 samples.



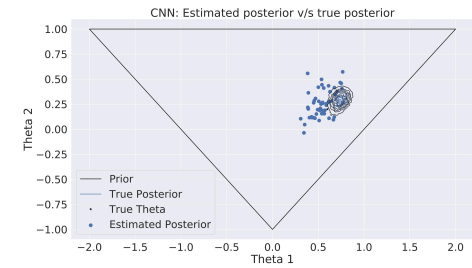
(f) CNN - training set of 10000 samples.



(g) DNN - training set of 100000 samples.



(h) PEN - training set of 100000 samples.



(i) CNN - training set of 100000 samples.

Figure 2: MA2 model: Estimated posterior compared to true posterior for each ANN architecture.

Network Type	MAE	$E\%$	MAE_{true}	$E\%_{true}$
Training Set Size 1000				
<i>DNN</i>	0.471 ± 0.023	0.676 ± 0.037	0.331 ± 0.206	0.464 ± 0.282
<i>PEN</i> ₁₀	0.341 ± 0.010	0.499 ± 0.133	0.246 ± 0.119	0.326 ± 0.172
<i>CNN</i>	0.378 ± 0.124	0.531 ± 0.180	0.287 ± 0.090	0.376 ± 0.086
Training Set Size 10,000				
<i>DNN</i>	0.319 ± 0.007	0.474 ± 0.010	0.280 ± 0.156	0.431 ± 0.262
<i>PEN</i> ₁₀	0.146 ± 0.004	0.221 ± 0.005	0.119 ± 0.073	0.173 ± 0.102
<i>CNN</i>	0.131 ± 0.004	0.198 ± 0.007	0.131 ± 0.071	0.189 ± 0.095
Training Set Size 100,000				
<i>DNN</i>	0.130 ± 0.003	0.197 ± 0.004	0.136 ± 0.074	0.200 ± 0.124
<i>PEN</i> ₁₀	0.106 ± 0.002	0.159 ± 0.003	0.105 ± 0.067	0.154 ± 0.102
<i>CNN</i>	0.122 ± 0.006	0.183 ± 0.009	0.129 ± 0.079	0.190 ± 0.122
Training Set Size 1,000,000				
<i>DNN</i>	0.104 ± 0.001	0.158 ± 0.002	0.107 ± 0.058	0.168 ± 0.095
<i>PEN</i> ₁₀	0.099 ± 0.002	0.149 ± 0.002	0.097 ± 0.047	0.154 ± 0.082
<i>CNN</i>	0.109 ± 0.006	0.165 ± 0.010	0.108 ± 0.053	0.176 ± 0.094

Table 1: MAE and $E\%$ for inference on the MA(2) model for training set sizes $10^3 - 10^6$. The values represent the mean and standard deviation over 10 independent experiments for each case.

The moving average model of order q , MA(q) [6] is defined for observations X_1, \dots, X_p as,

$$X_j = Z_j + \theta_1 Z_{j-1} + \theta_2 Z_{j-2} + \dots + \theta_q Z_{j-q}, j = 1, \dots, p,$$

where Z_j represent latent white noise error terms. This work considers $q = 2$ with experimental settings matching [6, 13] including $Z_j \sim N(0, 1)$. The MA(2) model is identifiable in the following triangular region,

$$\theta_1 \in [-2, 2], \theta_2 \in [-1, 1], \theta_2 \pm \theta_1 \geq -1.$$

The training data for all ANN architectures is sampled uniformly over this region. The training, validation and test set sizes are set to $10^6, 10^5, 10^5$ samples respectively, matching the configuration in [6]. The DNN architecture (3-layer, 100 neurons per layer) is also set to mirror the settings in [6]. The evolution of ANN model accuracy with varying size of training data is also explored, in addition to overall model accuracy over 10^6 training samples.

Table 1 compares the performance of the DNN, PEN and CNN architectures on the MA(2) model. The configuration for the PEN₁₀ variant follows [13]. The performance of all architectures is broadly comparable for the relatively simple MA(2) model. At a finer level, it can be observed that the PEN and CNN architectures outperform DNN across the board, especially for smaller training sets. As the training sets grow in size, the performance deficit between the architectures diminishes substantially.

A visual comparison of estimated posteriors is shown in Fig. 2. In order to estimate the posterior, the ABC reference table method was used with 0.01% acceptance ratio (50 samples accepted out of 500,000 trials). The training, test, validation and ABC trial data samples were consistent and the same across different architectures. In order to calculate the exact posterior distribution, the Random Walk Metropolis-Hastings method was used. Kernel Density Estimation (KDE) was used to visualize the exact posterior.

The posterior estimates in Fig. 2 reflect comparable performance between PEN and CNN architectures for larger training set sizes. The DNN architecture in comparison is less data-efficient with the posterior estimates consisting for larger variation from the true posterior. It can also be observed that 10,000 training samples are enough for the PEN and CNN architectures to be used as accurate high-quality summary statistics.

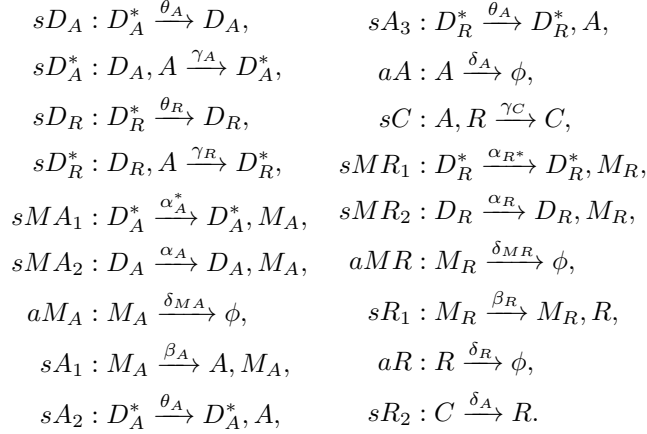
5.2 A Genetic Oscillator

A complex biochemical reaction network with oscillatory behavior due to Vilar et al. [12] is now considered. The network involves 9 species undergoing 18 reactions parameterized by 15 reaction constants. Let $\mathcal{S} = \{D_A, D_A^*, M_A, D_R, D_R^*, M_R, C, A, R\}$ be the set of species with initial copy numbers $\{1, 0, 0, 1, 0, 0, 10, 10, 10\}$

Parameters	α_A	α'_A	α_R	α'_R	β_A	β_R	δ_{MA}	δ_{MR}	δ_A	δ_R	γ'_A	γ_R	γ_C	θ_A	θ_R
dmin	0.0	100	0.0	20	10	1.0	1.0	0	0.0	0.0	0.5	0.0	0.0	0.0	0.0
dmax	80	600	4.0	60	60	7.0	12	2.0	3.0	0.7	2.5	4.0	3.0	70	300

Table 2: The uniform prior used for the genetic oscillator test problem.

respectively. The model involves the following reactions,



The first part of the experiments focuses on the accuracy of the summary statistics/predicted parameters $\hat{\theta}$ over the prior domain. As a baseline, we consider the time series of the single species C over a uniform prior bounded by **dmin**, **dmax** defined in Table 2.

To investigate the performance of the approach we conducted a series of numerical experiments. First, we compare the three architectures in terms of inference accuracy and training cost. Then, for the CNN, we consider a number of scenarios related both to experimental setup and to the cost of simulation. We vary the participating species and the amount of observed data, and we also look at the impact of the amount of simulated training data on the performance.

5.2.1 Comparison of the three network architectures

Table 3 lists the posterior mean estimation error (MAE and $E\%$) for the DNN, PEN and CNN architectures. The error estimates are calculated over 100,000 test points. The training, test and validation samples are consistent over the three architectures. It can be observed that the CNN outperforms the PEN and the DNN architectures for each of the 15 parameters. Interestingly, it can be observed that certain parameters like α'_A and θ_R are particularly hard to infer. It can also be seen that certain parameters like γ_A may not incur a large absolute inference error in terms of MAE, but $E\%$ values indicate that inferred results are not substantially better than optimal guessing.

Table 4 lists the training times and model sizes of the different ANN architectures. The DNN is the fastest but also the least informative of the three architectures. The results from the PEN₁₀ and the CNN are comparable with the CNN having a slight edge. The CNN had also the slowest training time and largest number of trainable parameters. In order to optimize the structure of each architecture, varying scales of networks were explored until the error rates converged.

5.2.2 Effect of different observations and data richness

Table 5 lists the posterior estimation error values in terms of $E\%$ corresponding to each specie (single subsets). This entails training one CNN model for each specie. It can be seen that specie C results in overall least error in estimating the posterior mean. However, certain species are more informative towards inferring certain parameters, which is intuitive considering specie-parameter reaction relationships within the genetic oscillator. For example, the parameter δ_A directly controls the deterministic dynamics of specie C , and this is reflected in Table 5 by δ_A having the lowest error when inferred by observing Specie C .

Table 6 lists the posterior estimation error when a subset of two species is used for estimation. Again, considering the specie-parameter relationships with respect to the reactions occurring within the genetic oscillator, certain specie combinations are more effective towards inferring certain (corresponding) parameters. The mean error values for all subsets are similar for two-sized subsets.

Parameters	Neural network architectures					
	DNN		PEN ₁₀		CNN	
	MAE	E%	MAE	E%	MAE	E%
α_A	12.779	0.639	8.035	0.402	7.832	0.392
α'_A	93.022	0.744	66.457	0.532	63.971	0.512
α_R	0.990	0.990	0.938	0.938	0.920	0.920
α'_R	8.899	0.890	7.900	0.790	7.583	0.758
β_A	10.454	0.836	6.532	0.523	6.315	0.505
β_R	1.037	0.691	0.772	0.514	0.735	0.490
δ_{MA}	2.115	0.769	1.393	0.507	1.359	0.494
δ_{MR}	0.283	0.566	0.213	0.425	0.201	0.403
δ_A	0.446	0.594	0.192	0.256	0.191	0.255
δ_R	0.136	0.774	0.070	0.399	0.064	0.366
γ_A	0.486	0.972	0.443	0.886	0.434	0.867
γ_R	0.922	0.922	0.806	0.806	0.786	0.786
γ_C	0.674	0.899	0.483	0.644	0.456	0.608
θ_A	15.871	0.907	10.967	0.627	10.525	0.601
θ_R	69.803	0.931	62.442	0.833	61.406	0.819
mean	14.528	0.808	11.176	0.605	10.852	0.585

Table 3: MAE and mean $E\%$ over the prior range for different ANN architectures for inferring time series responses of specie C. Error estimates are calculated over a test set of 100,000 $(\hat{\theta}(\mathbf{y}), \theta)$ tuples, $\theta \sim p(\theta)$.

Architecture	Training Time (hh:mm)	no. of parameters	
		Total	Trainable
DNN	00:26	457,167	450,767
PEN ₁₀	03:32	385,727	383,327
CNN	03:56	492,415	490,015

Table 4: Training time and the number of trainable parameters for each architecture. The training set size was 300,000 data samples, with a validation set of 20,000 samples.

Parameters	Species								
	D_a	D'_a	M_a	D_r	D'_r	M_r	C	A	R
α_A	0.770	0.772	0.315	0.820	0.820	0.763	0.387	0.518	0.563
α'_A	0.820	0.818	0.328	0.834	0.836	0.801	0.507	0.501	0.593
α_R	0.973	0.973	0.969	0.975	0.974	0.451	0.917	0.949	0.868
α'_R	0.956	0.956	0.950	0.956	0.956	0.460	0.758	0.913	0.895
β_A	0.887	0.886	0.813	0.889	0.889	0.859	0.505	0.449	0.581
β_R	0.892	0.891	0.880	0.899	0.899	0.856	0.485	0.778	0.749
δ_{MA}	0.853	0.852	0.297	0.861	0.861	0.831	0.493	0.464	0.529
δ_{MR}	0.789	0.790	0.773	0.799	0.801	0.144	0.396	0.658	0.607
δ_A	0.715	0.718	0.591	0.718	0.717	0.700	0.252	0.386	0.368
δ_R	0.695	0.688	0.635	0.697	0.699	0.568	0.364	0.464	0.374
γ_A	0.909	0.908	0.866	0.966	0.965	0.946	0.866	0.800	0.824
γ_R	0.969	0.970	0.960	0.790	0.790	0.794	0.781	0.901	0.896
γ_C	0.815	0.815	0.684	0.848	0.847	0.826	0.614	0.547	0.377
θ_A	0.746	0.751	0.615	0.886	0.883	0.833	0.597	0.590	0.560
θ_R	0.975	0.975	0.968	0.782	0.782	0.746	0.825	0.898	0.890
mean	0.851	0.851	0.710	0.848	0.848	0.705	0.583	0.654	0.645

Table 5: $E\%$ for posterior estimated mean using a CNN model trained corresponding to each single specie. Time vector $t = \{0 : 200 : 0.5\}$, training set size is 300,000 data samples. Results are calculated on a test set of 100,000 $(\hat{\theta}(\mathbf{y}), \theta)$ tuples, $\theta \sim p(\theta)$.

Parameters	Species						
	$\{M_a, C\}$	$\{D_r, M_r\}$	$\{M_r, C\}$	$\{M_r, A\}$	$\{C, A\}$	$\{C, R\}$	$\{A, R\}$
α_A	0.323	0.741	0.420	0.546	0.362	0.418	0.471
α'_A	0.357	0.793	0.561	0.544	0.423	0.544	0.475
α_R	0.925	0.472	0.473	0.449	0.902	0.731	0.864
α'_R	0.771	0.404	0.462	0.450	0.762	0.711	0.883
β_A	0.258	0.856	0.607	0.549	0.462	0.579	0.497
β_R	0.519	0.822	0.153	0.330	0.508	0.428	0.723
δ_{MA}	0.306	0.827	0.591	0.550	0.470	0.564	0.485
δ_{MR}	0.421	0.188	0.190	0.188	0.397	0.312	0.598
δ_A	0.170	0.680	0.299	0.421	0.236	0.291	0.327
δ_R	0.384	0.566	0.258	0.377	0.335	0.169	0.313
γ_A	0.851	0.947	0.875	0.831	0.754	0.820	0.778
γ_R	0.787	0.743	0.723	0.679	0.759	0.748	0.856
γ_C	0.622	0.802	0.630	0.607	0.413	0.388	0.294
θ_A	0.602	0.824	0.640	0.624	0.516	0.584	0.536
θ_R	0.814	0.735	0.722	0.678	0.794	0.760	0.855
mean	0.541	0.693	0.507	0.521	0.539	0.536	0.597

Table 6: $E\%$ for posterior estimated mean using a CNN model trained corresponding to 2-sized specie subsets. Only subsets with the lowest error on a parameters are shown. Time vector $t = \{0 : 200 : 1\}$, training set size is 300,000 data samples. Results are calculated on a test set of 100,000 $(\hat{\theta}(\mathbf{y}), \theta)$ tuples, $\theta \sim p(\theta)$.

parameters	nr. of training points							
	30k		100k		200k		300k	
	MAE	$E\%$	MAE	$E\%$	MAE	$E\%$	MAE	$E\%$
α_A	9.119	0.456	8.213	0.411	7.897	0.395	7.832	0.392
α'_A	77.965	0.624	66.956	0.536	65.181	0.521	63.971	0.512
α_R	0.975	0.975	0.937	0.937	0.925	0.925	0.920	0.920
α'_R	8.835	0.883	7.782	0.778	7.627	0.763	7.583	0.758
β_A	7.506	0.601	6.649	0.532	6.411	0.513	6.315	0.505
β_R	0.899	0.600	0.764	0.509	0.737	0.491	0.735	0.490
δ_{MA}	1.556	0.566	1.410	0.513	1.369	0.498	1.359	0.494
δ_{MR}	0.252	0.503	0.213	0.427	0.201	0.403	0.201	0.403
δ_A	0.241	0.321	0.205	0.274	0.196	0.261	0.191	0.255
δ_R	0.082	0.466	0.069	0.397	0.066	0.377	0.064	0.366
γ_A	0.471	0.942	0.442	0.884	0.436	0.872	0.434	0.867
γ_R	0.867	0.867	0.802	0.802	0.790	0.790	0.786	0.786
γ_C	0.545	0.726	0.485	0.646	0.466	0.621	0.456	0.608
θ_A	12.217	0.698	10.921	0.624	10.614	0.606	10.525	0.601
θ_R	67.207	0.896	62.933	0.839	61.963	0.826	61.406	0.819
mean	12.582	0.675	11.252	0.607	10.992	0.591	10.852	0.585

Table 7: Mean deviation in $E\%$ and inference error over the prior range for different sizes of training data. Results given on a test set of 100,000 $(\hat{\theta}(\mathbf{x}), \theta)$ tuples, $\theta \sim p(\theta)$.

Table 7 depicts the relationship between the size of the training set and inference error in the form of MAE and $E\%$. The largest training set size (300,000 samples) leads to least error, but the gains delivered over a training set of 200,000 samples are not significant. The most significant step up in inference accuracy is reflected when moving from a training set of 30,000 samples to 100,000 samples. For the considered test problem, the training set size of 100,000 samples appears to strike a fine balance between error in estimating the posterior mean and required training set size.

The relationship between simulation resolution (in terms of temporal sampling frequency or step size) and inference error is depicted in Table 8. As the step size increases, so does the inference error. This is intuitive as higher temporal resolution allows the convolution operator to characterize more detailed and accurate features over the input time series. This allows the CNN to incorporate more degrees of differentiation between the fine patterns present within time series from the genetic oscillator, and how they affect parameters θ .

Another interesting relationship to study is between the simulation length and inference error. Table 9 charts the evolution of inference error with increasing simulation length (from 25h to 200h). The results are intuitive as longer simulation lengths will incorporate distinct repeating temporal patterns more often, providing better discrimination abilities to the CNN. The test problem of the genetic oscillator consists of one oscillation every 24 hours, and so for a time range of 200 hours, 8 oscillations will be observed. It can be seen that for challenging parameters like α'_A , longer simulation lengths can enable significant gains in inference accuracy.

parameters	time step (h)									
	0.5		1.0		2.0		4.0		8.0	
	MAE	E%	MAE	E%	MAE	E%	MAE	E%	MAE	E%
α_A	7.832	0.392	8.396	0.420	9.155	0.458	10.091	0.505	10.933	0.547
α'_A	63.971	0.512	70.903	0.567	78.057	0.624	86.209	0.690	93.498	0.748
α_R	0.920	0.920	0.943	0.943	0.961	0.961	0.978	0.978	0.990	0.990
α'_R	7.583	0.758	7.795	0.779	8.051	0.805	8.573	0.857	9.184	0.918
β_A	6.315	0.505	7.661	0.613	8.932	0.715	9.819	0.786	10.391	0.831
β_R	0.735	0.490	0.789	0.526	0.873	0.582	1.022	0.681	1.169	0.779
δ_{MA}	1.359	0.494	1.651	0.600	1.870	0.680	2.001	0.728	2.118	0.770
δ_{MR}	0.201	0.403	0.220	0.439	0.251	0.501	0.306	0.612	0.363	0.727
δ_A	0.191	0.255	0.229	0.306	0.290	0.387	0.371	0.495	0.443	0.591
δ_R	0.064	0.366	0.071	0.405	0.083	0.477	0.104	0.597	0.128	0.734
γ_A	0.434	0.867	0.451	0.902	0.464	0.928	0.479	0.958	0.487	0.975
γ_R	0.786	0.786	0.804	0.804	0.837	0.837	0.888	0.888	0.931	0.931
γ_C	0.456	0.608	0.517	0.690	0.566	0.755	0.623	0.830	0.665	0.887
θ_A	10.525	0.601	11.727	0.670	12.866	0.735	14.184	0.811	15.271	0.873
θ_R	61.406	0.819	63.787	0.850	66.814	0.891	70.436	0.939	72.702	0.969
mean	10.852	0.585	11.730	0.634	12.671	0.689	13.739	0.757	14.618	0.818

Table 8: $E\%$ and inference MAE for training data with simulations of varying time steps. Results given on a test set of 100,000 $(\hat{\theta}(\mathbf{x}), \theta)$ tuples, $\theta \sim p(\theta)$.

parameters	time range (h)							
	25		50		100		200	
	MAE	E%	MAE	E%	MAE	E%	MAE	E%
α_A	12.436	0.622	10.547	0.527	9.089	0.454	7.832	0.392
α'_A	89.525	0.716	80.513	0.644	71.999	0.576	63.971	0.512
α_R	0.980	0.980	0.964	0.964	0.946	0.946	0.920	0.920
α'_R	8.482	0.848	8.240	0.824	7.962	0.796	7.583	0.758
β_A	9.111	0.729	8.152	0.652	7.269	0.582	6.315	0.505
β_R	0.890	0.593	0.841	0.560	0.795	0.530	0.735	0.490
δ_{MA}	2.039	0.742	1.810	0.658	1.582	0.575	1.359	0.494
δ_{MR}	0.245	0.489	0.230	0.461	0.217	0.433	0.201	0.403
δ_A	0.360	0.480	0.280	0.373	0.226	0.301	0.191	0.255
δ_R	0.131	0.750	0.099	0.566	0.077	0.443	0.064	0.366
γ_A	0.476	0.951	0.465	0.930	0.451	0.902	0.434	0.867
γ_R	0.879	0.879	0.846	0.846	0.812	0.812	0.786	0.786
γ_C	0.610	0.814	0.552	0.736	0.506	0.675	0.456	0.608
θ_A	14.771	0.844	13.298	0.760	11.891	0.680	10.525	0.601
θ_R	67.673	0.902	65.830	0.878	63.900	0.852	61.406	0.819
mean	13.907	0.756	12.844	0.692	11.848	0.637	10.852	0.585

Table 9: $E\%$ and inference MAE for training data with simulations of varying lengths. Results given on a test set of 100,000 $(\hat{\theta}(\mathbf{x}), \theta)$ tuples, $\theta \sim p(\theta)$.

Parameters	All	AS	CNN
α_A	20.172	27.553	4.377
α'_A	121.881	113.063	20.203
α_R	1.784	1.935	1.137
α'_R	9.967	9.311	3.728
β_A	16.905	16.113	4.071
β_R	1.742	1.821	0.466
δ_{MA}	4.991	4.542	0.853
δ_{MR}	0.391	0.482	0.062
δ_A	0.651	0.664	0.045
δ_R	0.165	0.172	0.048
γ'_A	0.605	0.609	0.271
γ_R	1.384	1.261	0.864
γ_C	0.590	0.701	0.306
θ_A	19.045	19.585	5.284
θ_R	88.125	84.123	65.694
mean	19.227	18.796	7.161

Table 10: MAE over the prior range for inferring time series responses of specie C using ABC with summary statistics selected using approximate sufficiency (AS) versus CNN. Error estimates are calculated on the well-known reference point.

Statistic	sum val.	median	mean	std. dev.	var.	max	burstiness
Frequency	0	6	5	6	14	3	17

Table 11: The frequency of selection of each summary statistic over 50 invocations of the approximate sufficiency (AS) algorithm.

Table 10 compares the ABC inference quality using the CNN-based summary statistic against the established approximate sufficiency (AS) method [7]. For reference, ABC inference using the complete pool of available summary statistics is also shown. The candidate pool of summary statistics is shown in Table 11 and includes mean, median, sum of values, standard deviation, variance, max and burstiness [4]. The most frequently selected statistics are variance and burstiness, and were used for performing ABC inference in conjunction with AS for results depicted in Table 10. It can be seen that using all statistics results in mean MAE of 19.227, while using AS improves it slightly to 18.796. The CNN-based summary statistic however, results in a substantial improvement, more than halving the MAE. The results also serve to highlight the advantage of the proposed method (and of estimated posterior mean in general as a summary statistic) in cases where the candidate pool of statistics itself might not contain sufficient discriminative ability to allow high quality inference. In such cases, using a highly expressive approximator of the posterior mean (such as the CNN) allows automatic learning of high fidelity summary statistics. Based on the results obtained on the two test problems, it can be seen that on the high-dimensional Vilar example, the proposed CNN architecture offers significant gains over the current state-of-the-art.

6 Conclusion

This paper presented the convolutional neural networks architecture for learning summary statistics for use in approximate Bayesian computation. In general, the proposed summary statistic learning framework can be used in any likelihood-free parameter inference framework that makes use of summary statistics to compare observed data and simulated responses. The network learns the mapping from time series responses $\mathbf{y} = f(\theta)$ to control parameters θ , which effectively represents the learned summary statistics. The proposed convolutional architecture is compared to state-of-the-art deep neural network and partially exchangeable network architectures. The convolutional architecture is shown to offer significant performance gains over competing architectures on a challenging high-dimensional test problem of a stochastic genetic oscillator. The convolutions act as filters to identify rich distinctive patterns in input time series \mathbf{y} and allow better characterization of θ given a specific \mathbf{y} . A simpler test problem of the moving averages model is also considered, where the competing architectures perform comparably. The proposed architecture is shown to be robust and versatile with respect to varying problem complexity and training set size.

References

- [1] Mark A Beaumont, Wenyang Zhang, and David J Balding. Approximate bayesian computation in population genetics. *Genetics*, 162(4):2025–2035, 2002.
- [2] Jean-Marie Cornuet, Filipe Santos, Mark A Beaumont, Christian P Robert, Jean-Michel Marin, David J Balding, Thomas Guillemaud, and Arnaud Estoup. Inferring population history with diy abc: a user-friendly approach to approximate bayesian computation. *Bioinformatics*, 24(23):2713–2719, 2008.
- [3] Paul Fearnhead and Dennis Prangle. Constructing summary statistics for approximate bayesian computation: semi-automatic approximate bayesian computation. *Journal of the Royal Statistical Society: Series B (Statistical Methodology)*, 74(3):419–474, 2012.
- [4] K-I Goh and A-L Barabási. Burstiness and memory in complex systems. *EPL (Europhysics Letters)*, 81(4):48002, 2008.
- [5] Ian Goodfellow, Yoshua Bengio, and Aaron Courville. *Deep learning*. MIT press, 2016.
- [6] Bai Jiang, Tung-Yu Wu, Charles Zheng, and Wing H. Wong. Learning summary statistic for approximate bayesian computation via deep neural network. *Statistica Sinica*, 27(4):1595–1618, 2017. ISSN 10170405, 19968507. URL <http://www.jstor.org/stable/26384090>.
- [7] Paul Joyce and Paul Marjoram. Approximately sufficient statistics and bayesian computation. *Statistical applications in genetics and molecular biology*, 7(1), 2008.
- [8] Jean-Michel Marin, Pierre Pudlo, Christian P Robert, and Robin J Ryder. Approximate bayesian computational methods. *Statistics and Computing*, 22(6):1167–1180, 2012.
- [9] Mijung Park, Wittawat Jitkrittum, and Dino Sejdinovic. K2-abc: Approximate bayesian computation with kernel embeddings. In *Artificial Intelligence and Statistics*, pages 398–407, 2016.
- [10] Dennis Prangle, Paul Fearnhead, Murray P Cox, Patrick J Biggs, and Nigel P French. Semi-automatic selection of summary statistics for abc model choice. *Statistical applications in genetics and molecular biology*, 13(1):67–82, 2014.
- [11] Scott A Sisson, Yanan Fan, and Mark Beaumont. *Handbook of approximate Bayesian computation*. Chapman and Hall/CRC, 2018.
- [12] José MG Vilar, Hao Yuan Kueh, Naama Barkai, and Stanislas Leibler. Mechanisms of noise-resistance in genetic oscillators. *Proceedings of the National Academy of Sciences*, 99(9):5988–5992, 2002.
- [13] Samuel Wqvist, Pierre-Alexandre Mattei, Umberto Picchini, and Jes Frellsen. Partially exchangeable networks and architectures for learning summary statistics in approximate bayesian computation. In *International Conference on Machine Learning*, pages 6798–6807, 2019.
- [14] Manzil Zaheer, Satwik Kottur, Siamak Ravanbakhsh, Barnabás Póczos, Ruslan Salakhutdinov, and Alexander J. Smola. Deep sets. *CoRR*, abs/1703.06114, 2017. URL <http://arxiv.org/abs/1703.06114>.
- [15] Yi-Tong Zhou and Rama Chellappa. Computation of optical flow using a neural network. In *IEEE International Conference on Neural Networks*, volume 1998, pages 71–78, 1988.